

# PHOTOCATALYTIC DEGRADATION OF SULFAMETHOXAZOLE BY TiO<sub>2</sub>/HAP COMPOSITE WITH UV-A IRRADIATION AND DEVELOPMENT OF RESPONSE SURFACE METHODOLOGY (RSM)

Chun SY<sup>1</sup>, Lee SJ<sup>1</sup>, Kim JT<sup>2</sup>, Chang SW<sup>1\*</sup>

<sup>1</sup> Department of Environmental Energy Systems Engineering, Kyonggi Univ., Suwon, Korea; <sup>2</sup> R&D Center for Advanced Technology of Wastewater Treatment and Reuse, Kyonggi Univ., Suwon, Korea

## 1. Introduction

The Sulfamethoxazole (SMX) is one of the non-degradable pollutants in aqueous medium that might not be treatable in the traditional biological treatment system, because of its antibacterial nature (Alexy et al., 2004). It is believed that SMX is not readily biodegradable in the WWTP, although other studies concluded that the SMX has the potential to be biodegraded with considerable dependence on a very long time of residence (Azéma et al., 2011). Alexy et al., (2004) also reported the bio-degradation of SMX was up to 27% after 28 days. Thus, the continuous discharge of SMX in the ecosystem could cause adverse effects of the more harmful bacteria which enhance the resistance to antibiotics (Jørgensen et al., 2000).

Advanced oxidation processes (AOPs) have been considered as treatment processes for a variety of non-biodegradable pollutants (Baetz et al., 1997; Wang, 2000; Neppolian et al., 2002; Kiriakidou et al., 1999). In general, AOPs utilize the formation of radicals that react with and destroy the target compounds. The common AOPs include ozone, UV/ozone, and UV/H<sub>2</sub>O<sub>2</sub>, which involve oxidation via the generated hydroxyl radical (•OH). The UV-A/TiO<sub>2</sub> processes are dependent upon several variables, including the initial SMX concentration, catalyst phase identity and dose, electron acceptor identity and the presence of non-target water constituents (Hu et al., 2007). Additionally, Degussa P-25 TiO<sub>2</sub> was mostly applied to degrade the SMX, and some works reported that biomaterials can be enhanced the photocatalytic activity of TiO<sub>2</sub>. Further, some studies reported about the SMX degradation by various treatment systems such as O<sub>3</sub>/UV, fenton, photo-fenton and other heterogeneous photocatalysis (González et al., 2007; Xekoukoulotakis et al., 2011; Hu et al., 2007; Abellán et al., 2009; Nasuhoglu et al., 2011).

In this study, the photocatalysis of antibiotics, SMX with TiO<sub>2</sub>/HAP composite (Titanium dioxide; TiO<sub>2</sub>, Hydroxyapatite; HAP), was utilized. The kinetics of SMX degradation by photocatalysis corresponding to different type of catalyst (HAP, Degussa P-25 TiO<sub>2</sub> and TiO<sub>2</sub>/HAP composite) was investigated to determine the enhanced photocatalytic activity. These were used to compare the effect of parameters from the results of statistical methods of RSM based on design of experiments (DOEs). Therefore, the objectives of this study were i) to synthesize the TiO<sub>2</sub>/HAP composite by sol-gel methods and ii) to observe potential of adsorption and photocatalysis onto TiO<sub>2</sub>/HAP system and iii) to optimize the UV/TiO<sub>2</sub>/HAP system with various operation parameters (e.g.; initial SMX concentration, initial dose of TiO<sub>2</sub>/HAP and irradiation intensity) by RSM under UV-A irradiation.

## 2. Materials and methods

The TiO<sub>2</sub>/HAP composite was prepared by sol-gel method using 2-propanol and TiO<sub>2</sub> as the starting materials and HNO<sub>3</sub> solution as the pH adjusting agent. Initially a 10 mM suspension of TiO<sub>2</sub> was prepared and stirred using magnetic stirrer. Then, about 10 mL of 2-propanol solution was added dropwise to the TiO<sub>2</sub> suspension. Following that, the pH of mixture suspension was adjusted to 1.5. After thoroughly mixing the reactants, the mixed solution was stirred at room temperature. Then, a 1 mM of HAP suspension was added to the transparent sol. The prepared suspension was evaporated for 2 hr using rotary evaporator. The prepared TiO<sub>2</sub>/HAP powder was formed by dry ball milling and calcinated in an oven at 500°C for 2 hr. Microstructure of the samples was studied using scanning electron microscopes by using a PHILIPHS XL30 scanning electron microscope operating at 10 kV. Furthermore, X-ray diffraction was conducted (using an X'Pert Powder X-ray diffractometer operating at 50 kV, 1 mA, Cu K<sub>α</sub> radiation, λ = 0.15406 nm) to determine the components in TiO<sub>2</sub>/HAP composite. The experimental conditions such as 1 L of total volume, 10 mg L<sup>-1</sup> of SMX initial concentration, 1000 mg L<sup>-1</sup> of TiO<sub>2</sub> (Degussa, P-25) or TiO<sub>2</sub>/HAP composite addition amount were kept constant throughout this work. The concentration of SMX, although considerably greater than those typically monitored in field or

environment, were chosen to consider the process efficiency within a certain time scale and the accurate analyzing of SMX photodegradation and mineralization with the analytical skills employed in this study. The batch reactor has a thermostatic condition and 1.5 L quartz beaker equipped with three lamps (length 22.5 cm), placed in its center (Philips TL 6W/05, UV-A), with nominal power of 6W each, which emitted radiation between 350 and 400 nm, with a maximum at 365 nm. At given irradiation time intervals, 10 mL of the reacted solution was sampled at sampling port by syringe and filtrated using syringe filter (PTFE model from Woongki Science Co. Ltd., Korea). The application of the RSM is permitted to establish a mathematical relationship between dependent and independent variables and the process optimization. The experimental data were fitted to a second-order polynomial equation as follows (Arslan-Alaton et al., 2009).

$$Y = b_0 + \sum_i^n b_i x_i + \sum_i^n b_{ii} x_i^2 + \sum_{j>i}^n \sum_{i=1}^n b_{ij} x_i x_j \quad (1)$$

Where  $Y$  refers to the response,  $x_i$  refers to the codified independent variables,  $b_0$  is the interception term,  $b_i$  determines the influence of the variable  $i$  in the response (linear term),  $b_{ii}$  is a parameter that determines the shape of the curve (quadratic effect) and  $b_{ij}$  corresponds to the effect of the interaction among variables  $i$  and  $j$ . To convert the natural variables ( $X_i$ ) into dimensionless codified values ( $x_i$ ), these conversions of variables were calculated using the following equation.

$$x_i = (X_i - X_0) / \Delta X \quad (2)$$

The statistical analysis proceeds with an ANOVA test, which evaluates the adequacy of the model fitting. The variations that occur in the response can be attributed to the model and are not due to random errors if the F-ratio is higher than the Fisher's F-value and consequently if the F-probability is less than 0.05 (for 95% confidence level). To determine which parameters and/or interactions have statistical meaning, the Student's t-test was used. If t-probability is smaller than 0.05, the parameter or interaction is significant. A factorial, the BBD for three factors with replicates at the center point, was used in the investigation. Experimental data analysis was developed using the Minitab 14.1 (USA) software and the statistical analysis was achieved by regression analysis and the ANOVA (analysis of variance) test at 95% confidence level. In this study, the experimental plan was carried out as a BBD consisting of 15 experiments.

### 3. Results and discussion

The TiO<sub>2</sub>/HAP composite was characterized by powder X-ray diffractometer (X'Pert Powder, Netherlands) using Ni-filtered Cu K $\alpha$  radiation in the range of 2 $\theta$  from 10° to 80°. As shown in Fig. 2a, the characteristic diffraction peaks of TiO<sub>2</sub>/HAP composite was confirmed that the main constituent of TiO<sub>2</sub> (anatase) and HAP which are the similar result as reported previously (Sun and Wang, 2008; Nathanael et al., 2010). In the XRD patterns, there was a presence of diffraction peaks corresponding to anatase, while the HAP phase of TiO<sub>2</sub>/HAP was also detected, indicating that photocatalytic activity and adsorption were performed in the anatase and HAP phases. Also, the surface morphology of TiO<sub>2</sub>/HAP composite was analyzed by SEM image. As shown in Fig. 2b, the grayish surface reveals that the TiO<sub>2</sub> is co-doped with HAP. Additionally, the morphologies on the surface of TiO<sub>2</sub>/HAP composite have a regular sphere surface. These XRD and SEM results agree with Wang et al. (2010) who reported that the enhanced photocatalytic activity of TiO<sub>2</sub>/HAP composite. However, the particle size of TiO<sub>2</sub>/HAP structure was smaller than Wang's (Wang et al., 2010) results which presented by SEM image of TiO<sub>2</sub>/HAP composite. Although, the synthesis procedure of TiO<sub>2</sub>/HAP was similar as co-doped the HAP method but it seems to be the molar ratio of TiO<sub>2</sub> and HAP and heat treatment condition were the reasons of different structure size. Photocatalytic experiments were conducted by various catalysts such as TiO<sub>2</sub> (Degussa P-25), HAP and TiO<sub>2</sub>/HAP that shows the photocatalytic activities of each catalysts under 240 min UV-A irradiation when a 10 mg L<sup>-1</sup> of SMX present in contact with 1 g L<sup>-1</sup> of each catalysts. Additionally, It is reported that the interaction between SMX molecule and TiO<sub>2</sub>-based photocatalytic materials is affected by both the surface properties of the photocatalyst and the structure of the target compounds (such as SMX) (Xu et al., 2012). Therefore, the adsorption experiments using Degussa P-25, HAP and TiO<sub>2</sub>/HAP were also carried out to determine the SMX reduction in the dark for 60 min stirring with near-neutral pH. For evaluating the adsorption and photocatalytic activities of Degussa P-25, HAP and TiO<sub>2</sub>/HAP composite, the conversion of SMX was performed by HPLC/MS. The result was displayed in Fig. 2c.

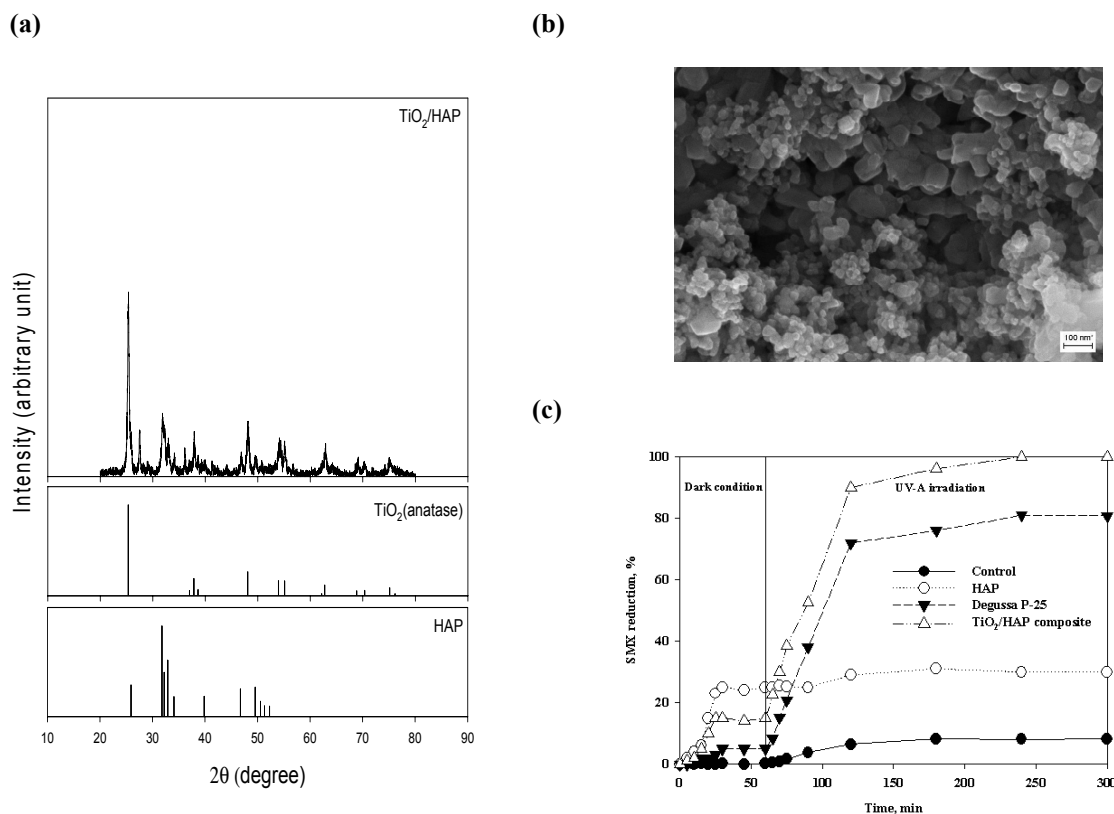


**Fig. 2.** Characterization results of TiO<sub>2</sub>/HAP composite at 500 °C for 120 min heat treatment (a) XRD pattern and (b) SEM image and (c) Relative activity of various catalysts for 10 mg L<sup>-1</sup> SMX for 60 min dark condition and 240 min UV-A irradiation

An analysis of variance (ANOVA) was performed on the experimental result to evaluate the effect of variables and the regression model for SMX degradation. The all terms of linear, quadratic and interaction were also significant at the both of SMX ( $Y_1$ ) and COD<sub>Cr</sub> reduction ( $Y_2$ ).

$$\text{SMX reduction (\%)} = 95.6 + 0.138X_2 + 2.675X_3 - 1.325X_1^2 - 0.475X_2^2 - 0.350X_3^2 - 0.725X_1X_3 + 0.725X_2X_3 \quad (3)$$

$$\text{COD}_{\text{Cr}} \text{ reduction (\%)} = 75.6 + 0.563X_1 + 2.500X_2 + 3.038X_3 - 1.375X_1^2 - 0.675X_3^2 + 0.625X_1X_2 - 1.100X_1X_3 + 1.075X_2X_3 \quad (4)$$

Eq. (3) and (4) present the models for SMX reduction (%) and COD<sub>Cr</sub> reduction (%) after excluding insignificant coefficients accordance with regression results. These models can be seen that SMX and COD<sub>Cr</sub> reduction increase with the TiO<sub>2</sub>/HAP dose ( $X_2$ ) and irradiation intensity ( $X_3$ ) but decrease with SMX concentration ( $X_1$ ). Especially, for the SMX reduction, the linear term of  $X_1$  was excluded cause of its insignificant. The interaction effect was observed at the terms of SMX concentration and irradiation intensity ( $X_1X_3$ ), and TiO<sub>2</sub>/HAP dose and irradiation intensity ( $X_2X_3$ ). The behavior of the process can be described by  $T$ -values and  $P$ -values. Surface plots (3D plot) of the response for the experimental factors are presented in Fig. 3. Surface plots (3D plot) were obtained based on effects of the three factors (SMX concentration, TiO<sub>2</sub>/HAP composite dose and irradiation intensity) at three levels. These surface plots obtained from the MINITAB 14.0 software (USA) provide a three dimensional (3D) plot of the SMX and COD<sub>Cr</sub> reduction with various conditions of each factors. Additionally, curvature (ridge of response surface) was observed that means the interaction term was significantly affected on SMX and COD<sub>Cr</sub> reduction. The plots indicate optimum conditions to be -0.9171 of SMX concentration ( $X_1$ ), 0.8702 of TiO<sub>2</sub>/HAP composite dose ( $X_2$ ) and 1.0 of irradiation intensity ( $X_3$ ) by coded

condition of variables. These conditions were converted to actual level as 5.4145 mg L<sup>-1</sup> of SMX, 1.4351 g L<sup>-1</sup> of TiO<sub>2</sub>/HAP composite dose and 18 W of irradiation intensity. The SMX and COD<sub>Cr</sub> reductions under these conditions were nearly 100% and 81.2%, respectively.

As a result, the TiO<sub>2</sub>/HAP composite dose has adverse effect on the SMX mineralization at above of 1.4 g L<sup>-1</sup> that is similar result of Fig. 3a. Especially, according with the regression equation, the SMX mineralization was observed to satisfy as above of 80% at the optimum condition of TiO<sub>2</sub>/HAP composite dose. Through a quantified comparison, the effect of SMX concentration onto mineralization was changed from 79% to 81% when the other condition was hold at optimum level. In contrast, the TiO<sub>2</sub>/HAP composite dose was affected on mineralization that changed from 74% to 80%, and the irradiation intensity observed also sensitive effect on mineralization that changed from 70% to 80%. These results show the quantified effects on the reaction by each parameter that the maximum SMX and COD<sub>Cr</sub> reductions are obtained with TiO<sub>2</sub>/HAP composite dose and irradiation intensity of nearly upper point of the range employed.

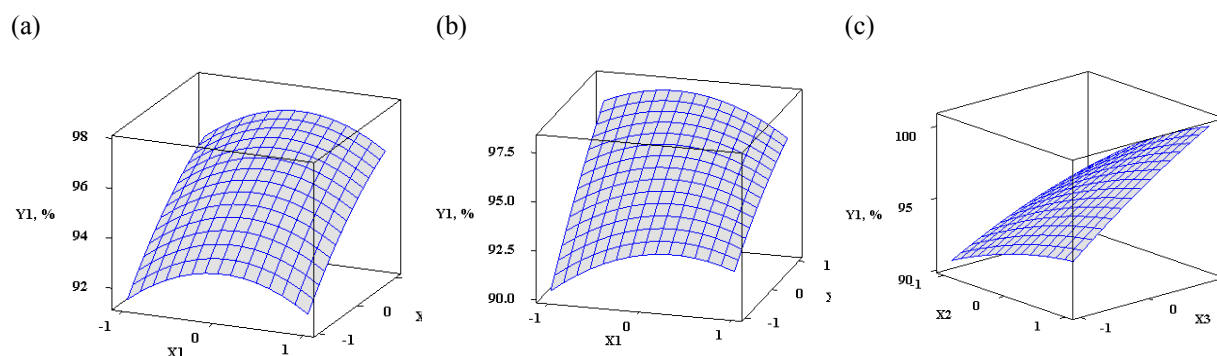


**Fig. 3. Response surface plot for SMX reduction (Y<sub>1</sub> : SMX reduction, X<sub>1</sub> : SMX concentration, X<sub>2</sub> : TiO<sub>2</sub>/HAP composite dose and X<sub>3</sub> : irradiation intensity)**

This study focused on evaluating the process optimization and for SMX reduction by TiO<sub>2</sub>/HAP composite with UV-A irradiation. The TiO<sub>2</sub>/HAP composite successfully decomposed the SMX nearly 100% and mineralized about 80%. The photocatalytic activity of TiO<sub>2</sub>/HAP composite has highly activity than Degussa P-25 TiO<sub>2</sub> cause of the synergy effect between TiO<sub>2</sub> and HAP. The enhanced photocatalytic activity was analyzed by *Langmuir-Hinselwood* kinetic model that present the  $k_{\text{photocatalysis+adsorption}}$  ( $k_r K$ ) was reflect a higher rate constant than HAP and Degussa P-25. The TiO<sub>2</sub>/HAP molar ratio was considered to find proper composition ratio. The SMX reduction and mineralization increase with the TiO<sub>2</sub> molar ratio increasing from 2.5 mM to 10 mM, and then slowly falls with the further increasing until 12.5 mM. In addition, the effect of TiO<sub>2</sub>/HAP dose and SMX concentration was performed to determine the range of factor on RSM. BBD result (regression analysis and ANOVA) was used to define the main effect and interaction with quantitative comparison. In addition, UV/TiO<sub>2</sub>/HAP system was optimized to maximize the SMX mineralization. The three factors (SMX concentration, TiO<sub>2</sub>/HAP dose and irradiation intensity) applied to define the response maximize at 5.4145 mg L<sup>-1</sup> of SMX, 1.4351 g L<sup>-1</sup> of TiO<sub>2</sub>/HAP composite dose and 18 W of irradiation intensity. Within the optimum conditions, SMX and COD<sub>Cr</sub> reductions achieved were nearly 100% and 81.2%, respectively. Hence, TiO<sub>2</sub>/HAP composite is recommended as an effective system for SMX degradation. Additionally, the TiO<sub>2</sub>/HAP composite with UV-A system is seems to be also useful for halogenated pollutants degradation and mineralization.

#### 4. Acknowledgements

This work was supported by the National Research Foundation of Korea(NRF) grant funded by the Korea government(MEST) (No. 2010-0010577)

#### 5. References

- [1] D. Nasuhoglu, V. Yargeau, D. Berk, *Journal of Hazardous Materials* 186 (2011), 67-75.
- [2] T. Herberer, *Journal of Hydrology* 266 (2002), 175-189.

- [3] P.E. Stackelberg, E.T. Furlong, M.T. Meyer, S.D. Zaugg, A.K. Henderson, D.B. Reissman, *Science of The Total Environment* 329 (2004), 99-113.
- [4] R. Alexy, T. Kumpel, D.K. Kummerer, *Chemosphere* 57 (2004), 505-512.
- [5] J. Azéma, B. Guidetti, A. Korolyov, R. Kiss, C. Roques, P. Constant, M. Daffé, M. Malet-Martino, *European Journal of Medicinal Chemistry* 46 (2011), 6025-6038.
- [6] L.A. Pe´rez-Estrada, M.I. Maldonado, W. Gernjak, A. Agu´era, A.R. Ferna´ndez-Alba, M.M. Ballesteros, S. Malato, *Catalysis Today* 101 (2005), 219-226.
- [7] K. Kummerer, *Chemosphere* 45 (2001), 957-969.
- [8] S.E. Jørgensen, B. Halling-Sørensen, *Chemosphere* 40 (2000), 691-699.
- [9] R.L. Baetz, M. Iangphasuk, *Chemosphere* 35 (1997), 585-596.
- [10] Y. Wang, *Water Research* 34 (2000), 990-994 .
- [11] B. Neppolian, H.C. Choi, S. Sakthivel, B. Arabindoo, V. Murugesan, *Journal of Hazardous Materials* 89 (2002), 303-317.
- [12] F. Kiriakidou, D.I. Kondarides, X.E. Verykios, *Catalysis Today* 54 (1999), 119-130.
- [13] C. Dominguez, J. Garcia, M.A. Pedraj, A. Torres, M.A. Galan, *Catalysis Today* 40 (1998), 85-101.
- [14] E. Pelizzetti, C. Minero, *Electrochimica Acta* 38 (1993), 47-55.
- [15] J.M. Herrmann, J. Didier, P. Pichat, S. Malato, S. Blanco, *Applied Catalysis B: Enviromental* 17 (1998), 15-23.
- [16] D.C. Schmelling, K.A. Gray, *Water Research* 29 (1995), 2651-2662.
- [17] A. Fujishima, X. Zhang, D.A. Tryk, *Surface Science Reports* 63 (2008), 515-582.
- [18] O. González, C. Sans, S. Esplugas, *Journal of Hazardous Materials* 146 (2007), 459-464.
- [19] N.P. Xekoukoulotakis, C. Drosou, C. Brebou, E. Chatzisymeon, E. Hapeshi, D. Fatta-Kassinou, D. Mantzavinos, *Catalysis Today* 161 (2011), 163-168.
- [20] L. Hu, P.M. Flanders, P.L. Miller, T.J. Strathmann, *Water Research* 41 (2007), 2612-2626.
- [21] M.M. Estrella, D.M. Fine, *Advances in Chronic Kidney Disease* 17 (2010), 26-35.
- [22] B. Bayarri, M.N. Abellán, J. Giménez, S. Esplugas, *Catalysis Today* 129 (2007), 231-239.
- [23] R.A. Palominos, A. Mora, M.A. Mondaca, M. Pérez-Moya, H.D. Mansilla, *Journal of Hazardous Materials* 158 (2008), 460-464.
- [24] M.N. Abellán, J. Giménez, S. Esplugas, *Catalysis Today* 144 (2009), 131-136.
- [25] Y. Hu, D. Li, Y. Zheng, W. Chen, Y. He, Y. Shao, X. Fu, G. Xiao, *Applied Catalysis B: Environmental* 104 (2011), 30-36.
- [26] I. Arslan-Alaton, T. Olmez-Hanci, B.H. Gursoy, G. Tureli, *Chemosphere* 76 (2009), 587-594.
- [27] M. Tsukada, M. Wakamura, N. Yoshida, T. Watanabe, *Journal of Molecular Catalysis A: Chemical* 338 (2011), 18-23.
- [28] N. Ma, Y. Zhang, X. Quan, *Water research* 44 (2010), 6104-6114.
- [29] M.P. Reddy, A. Venugopal, M. Subrahmanyam, *Applied catalysis B: Environmental* 69 (2007), 164-170.
- [30] S. Fukahori, T. Fujiwara, R. Ito, Naoyuki Funamizu, *Desalination* 275 (2011), 237-242.
- [31] P.i Wang, H. Yi-Liang, H. Ching-Hua, *Diagnostic Microbiology and Infectious Disease* 67 (2010), 1-8.
- [32] L. Xu, G. Wang, F. Ma, Y. Zhao, N. Lu, Y. Guo and X. Yang, *Applied surface science*, 258 (2012), 7039-7046.
- [33] Q. Yang, Y. Zhang, M. Liu, M. Ye, Y.Q. Zhang and S. Yao, *Analytica Chimica Acta*, 597 (2007), 58-66.